Polymer 54 (2013) 6501–6509

Contents lists available at ScienceDirect

Polymer

journal homepage: www.elsevier.com/locate/polymer

Feature article

Low band gap polymers for photovoltaic device with photocurrent response wavelengths over 1000 nm

Erjun Zhou [a], Kazuhito Hashimoto [b,**], Keisuke Tajima [a,c,*]

[a] RIKEN Center for Emergent Matter Science (CEMS), 2-1 Hirosawa, Wako 351-0198, Japan
[b] Department of Applied Chemistry, School of Engineering, The University of Tokyo, 7-3-1 Hongo, Bunkyo-ku, Tokyo 113-8656, Japan
[c] Japan Science and Technology Agency (JST), Precursory Research for Embryonic Science and Technology (PRESTO), 4-1-8 Honcho, Kawaguchi, Saitama 332-0012, Japan

ARTICLE INFO

Article history:
Received 25 July 2013
Received in revised form
20 September 2013
Accepted 28 September 2013
Available online 5 October 2013

Keywords:
Bulk-heterojunction
Conjugated polymers
Low band gap
Photovoltaic
Polymer solar cells

ABSTRACT

To pursue high power conversion efficiency (PCE) of polymer solar cells (PSCs), many new semiconducting polymers with low band gaps have been developed in the past several years. In this perspective paper, we focused on super low band gap photovoltaic polymers with photocurrent response extending over 1000 nm. This kind of micrometer-response polymers (μmR-polymer) could increase the short circuit current (J_{SC}) due to better match of absorption spectra of the polymers with the solar irradiation and show tremendous potential for application in tandem solar cells and transparent solar cells. The necessary conditions for the design of this kind of μmR-polymers are discussed. Furthermore, the remaining problems and challenges, and the key research direction in near future are discussed.

1. Introduction

Over the past two decades, polymer solar cells (PSCs) have received a great deal of attention as a potential alternative to silicon-based solar cells because of PSCs having the unique advantages of low cost, light weight, energy-saving fabrication processes, and applicability in flexible large-area devices [1–8]. Bulk-heterojunction (BHJ) devices were first reported in 1995 [9] and consist of a conjugated polymer (electron donor) and fullerene derivative (electron acceptor); the development of BHJ devices has greatly enhanced the power conversion efficiency (PCE) of PSCs under sunlight.

Generally, the energy conversion from light energy to electrical energy in BHJ PSCs comprised of five fundamental steps: 1) harvesting of photons by chromophores (donor or acceptor) to generate excitons, 2) diffusion of the excitons to the interface of donor and acceptor, 3) dissociation of the excitons into free charge carriers, 4) transportation of the free charge carriers toward the corresponding electrodes, and 5) charge collection at electrodes. Thus, the overall performance of PSCs could be improved through research focused on two different approaches: optimization of device fabrication and development of new materials to facilitate the above five steps. The former approach includes optimization of the solvent, molecular additives, solution concentration, donor/acceptor ratio, spin-coating rate during deposition, drying temperature, and annealing conditions. On the other hand, the choice of the photovoltaic polymers also has a crucial effect on photovoltaic performance. Among the large variety of photovoltaic polymers, regioregular poly(3-hexylthiophene) (P3HT) has been studied as a "benchmark" electron donor material. BHJ photovoltaic devices with a mixture of P3HT and [6,6]-phenyl C_{61} butyric acid methyl ester (PCBM) have been reported to have PCEs as high as 5% [10,11]. Structural modification of polythiophene derivatives has also been extensively investigated [12–18]. However, for devices utilizing such polythiophene derivatives, it appears that the upper limit on PCE has been reached because the large mismatch between the relatively large band gap (~2.0 eV) and solar spectrum leads to insufficient light absorption, limiting further improvement of the photocurrent. Hence, it is essential to lower the band gap of photovoltaic polymers such that the absorption band is shifted toward longer wavelengths.

* Corresponding author. RIKEN Center for Emergent Matter Science (CEMS), 2-1 Hirosawa, Wako 351-0198, Japan.
** Corresponding author.
E-mail addresses: hashimoto@light.t.u-tokyo.ac.jp (K. Hashimoto), keisuke.tajima@riken.jp (K. Tajima).

0032-3861/$ – see front matter © 2013 Elsevier Ltd. All rights reserved.
http://dx.doi.org/10.1016/j.polymer.2013.09.058

There are two successful and flexible strategies to design low band gap conjugated polymers, one is converting aromatic moieties to quinoid structures along the polymer backbone [19], another is to incorporate an electron-rich unit (donor) and electron-deficient unit (acceptor) into repeating units, forming internal donor–acceptor (D–A) structures [20,21]. The alternating D–A copolymer approach enables tuning of the optical and electronic properties of the resulting copolymer through intramolecular charge transfer (ICT) from the donor to the acceptor. Clearly, the rational selection of building blocks is critical to the realization of the well-defined control of the photophysical properties and frontier molecular orbital energy levels of the resulting copolymers to meet the requirements for BHJ-PSC applications. Therefore, various aromatic heterocycles were exploited to develop highly efficient donor polymers for BHJ-PSC applications.

For electron-donating building blocks, thiophene and benzene aromatic rings are the most important structural ingredients to construct these segments. Among them, tricyclic aromatic structures based on biphenyl or bithiophene with a bridging atom (C, S, Ge or N) have been extensively studied. Scheme 1 shows eight examples of donor segments, with their abbreviations: fluorene (F) [22–24], dibenzosilole (DBS) [25,26], dibenzogermole (DBG) [27], carbazole (C) [28–30], cyclopenta[2,1-*b*:3,4-*b*]dithiophene (CPDT) [31–34], dithienosilole (DTS) [35–37], dithienogermole (DTG) [38–41] and dithieno[3,2-*b*:2′,3′-*d*]pyrrole (DTP) [42–45].

On the other hand, the acceptor segment is often based on a pyrazine or thiadiazole unit with electron-deficient C=N bonds. Scheme 2 shows seven typical examples of acceptor segments with their abbreviations: 2,1,3-benzothiadiazole (BT), quinoxaline (Qx) [46–50], thieno[3,4-*b*]pyrazine (TP) [51–56], thieno[3,4-*c*][1,2,5]thiadiazole (TT) [57,58], pyrazino[2,3-*g*]quinoxaline (PQ) [59–61], [1,2,5]thiadiazolo[3,4-*g*]quinoxaline (TQ) [62–67], and benzo[1,2-*c*;3,4-*c*]bis[1,2,5]thiadiazole (BBT) [68–71].

A necessary requirement for a D–A type polymer to have promising photovoltaic performance is a proper combination of donor and acceptor segments such that the absorption spectrum of the polymer is matched to the solar spectrum. If we assume that a transparent electrode has a transmittance of 85%, from the standard spectrum of solar irradiation (AM 1.5G), the theoretical maximum of the short circuit current density (J_{SC}) of a PSC device is approximately 14.3 mA cm^{-2}, with a response range from 300 to 650 nm (when using the standard material P3HT). If the photocurrent response is extended to 800 nm, the theoretical maximum of J_{SC} can be increased to ~23.0 mA cm^{-2}; furthermore, if the response is extended to 1000 nm, the theoretical maximum of J_{SC} can be increased to ~31.9 mA cm^{-2}. These simple calculations clearly show that the absorption spectrum strongly affects photovoltaic performance, especially J_{SC}.

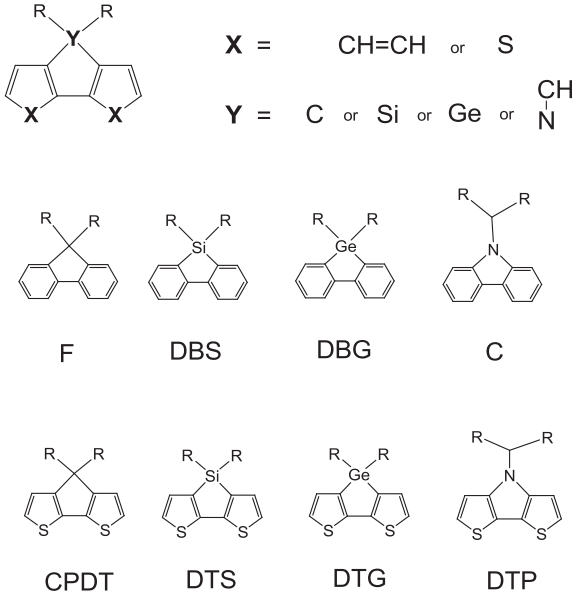

Scheme 1. Eight typical donor segments based on fused biphenyl or bithiophene units.

In reality, it is not practical to absorb the whole range of the spectrum with a single polymer material due to the limited absorption bandwidth. Since the solar spectrum have the maximum of the photon flux at around 700 nm, the semiconducting polymers with an absorption maximum at around 700 nm would have the highest matching of the spectra with single absorption band. This approach also enables a relatively high open-circuit voltage (V_{OC}), since a large difference between the HOMO and lowest unoccupied molecular orbital (LUMO) energies can be maintained for the acceptor material (PCBM). Recently, this strategy, along with rigorous device optimization, has been used to achieve considerable improvements in the performance of D–A copolymers. Certain polymers based on the building blocks described above, such as PDBS-DTBT[25], PC-DTBT[30], PCPDT-BT[32] and PDTS-BT[35], show relatively large J_{SC} (9.5–16.2 mA cm^{-2}) under sunlight, and the onset of the photocurrent response reaches 660–800 nm. These are only moderately red-shifted, by 10–150 nm, when compared with the adsorption onset of P3HT (~650 nm). Furthermore, V_{OC} can be kept at a high value, owing to the deep HOMO levels of the donor polymers. The delicate balance between these two factors results in high PCEs of 5–6%. There are a number of review articles that discuss D–A type photovoltaic polymers with absorption onsets up to 800 nm.

Up to now, this “balanced” strategy has given the best result, in terms of PCE, for single-layer BHJ PSCs. However, in consideration of the simple photocurrent calculation above, an alternative approach to achieving high performance may exist: aim for the highest J_{SC} by collecting as much of the photon flux as possible. In this manuscript, we focus on photovoltaic polymers with low band gaps whose optical absorption and photocurrent response extend to 1 μm. We call this type of polymer a “micrometer-response polymer” (μmR-polymer). μmR-polymers can utilize a larger proportion of the sunlight and have the possibility to obtain J_{SC} of over 30 mA cm^{-2}. They also have great promise for application in tandem photovoltaic cells in combination with polymers having larger band gaps and transparent solar cells that can be used for windows.

A tandem structure is equivalent to two cells connected in series, which offers a number of advantages: V_{OC} for a tandem cell is increased to the sum of V_{OC} for the two individual cells and the use of two semiconductors with different band gaps enables absorption over a broad range of photon energies within the solar emission spectrum. However, the current is limited by whichever cell has the lowest value. In addition, the overlap between the absorption spectra of the two cells decreases the efficiency of the tandem cells [72,73].

Thus, development of μmR-polymers with strong absorption in the range over 700 nm is very important to achieve promising tandem photovoltaic cells with higher PCE, after combining with effective moderate band gap polymers. In recent years, several research groups [74–79] focused on tandem devices and highest PCE over 10% have been achieved [80].

Furthermore, μmR-polymers should also be useful in polymer photodetector devices with high sensitivity in the near-infrared (NIR) region [81]. Additionally, the synthesis of μmR-polymers is a challenge and is a field that has been relatively less explored. We will firstly discuss the principles for designing polymers used in photovoltaic devices, and then review examples of photovoltaic

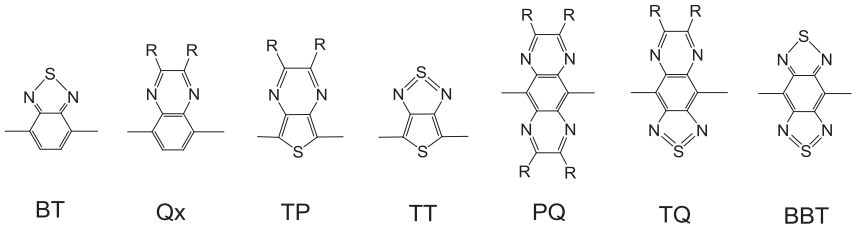

Scheme 2. Seven typical acceptor segments containing C=N bonds.

devices with these polymers. We summarize the current state of the art in μmR-polymers and conclude by discussing the prospects for this research field.

2. Design of μmR-polymers for PSCs

The fundamental requirements for promising photovoltaic polymers include (1) a broad absorption bandwidth, which enables more sunlight to be absorbed; (2) a low-lying HOMO to keep V_{OC} as high as possible, together with a suitable LUMO energy level to enable effective photoinduced charge transfer from the polymers to the acceptor in the BHJ device; (3) high carrier mobility to ensure that effective charge carrier transport to the electrodes suppresses photocurrent loss; and (4) good solubility, and appropriate compatibility with fullerene derivatives, in order to form high-quality films by solution processing.

For μmR-polymers, requirement (1) is well fulfilled due to the super low band gap (less than 1.24 eV). However, in regard to the energy level, it is a big challenge to fulfill both low-lying HOMO and suitable LUMO energy level simultaneously with one polymer, which might be one main reason for the lack of successful μmR-polymers.

For the D–A type copolymer approach, strong ICT from the donor segment to the acceptor unit is necessary to realize a μmR-polymer. Here, we classify the polymers according to their strong acceptor building blocks, which include TQ, TP, PQ, TT, diketo-pyrrolopyrrole (DPP), perylene diimide (PDI) and naphthalene diimide (NDI) (Table 1).

2.1. TQ-based μmR-polymers

As a strongly electron-deficient building block, TQ was introduced into photovoltaic polymers by Wang et al. in 2004, and the resulting material, **P1**, was the first example of a μmR-polymer [62]. **P1** shows optical absorption peaks in two wavelength ranges, 300–500 nm and 650–1000 nm. PSCs were fabricated in a traditional BHJ type sandwich structure of ITO/PEDOT:PSS/active layer/LiF/Al. When using PCBM as the acceptor, the PSCs exhibited V_{OC} of 0.69 V, J_{SC} of 0.53 mA cm^{-2}, and PCE of 0.17%. The low-lying LUMO energy level of **P1** (−4.0 eV) might have inhibited efficient photoinduced charge transfer. Thus, the PCBM was replaced with another fullerene derivative, 3′-(3,5-bis-trifluoromethylphenyl)-1′-(4-nitrophenyl)pyrazolino[60]fullerene (BTPF), which has a lower-lying LUMO (−4.1 eV). This **P1**:BTPF combination resulted in an increase in the PCE of the PSCs to 0.3%. In addition to the more effective photoinduced charge transfer, the improved morphology of the PSC network structure could also contribute to effective charge separation and transport. Atomic force microscopy studies of morphology showed that there was no obvious phase separation in the **P1**:BTPF films, whereas the **P1**:PCBM films had large phase separation, with domains sizes up to 10–20 μm when deposited by spin coating from solution. Furthermore, use of 3′-(3,5-bis-trifluoromethylphenyl)-1′-(4-nitrophenyl)pyrazolino[70]fullerene (BTPF70) as the accepter in combination with **P1** increased the PCE of the device to 0.7%. The external quantum efficiency (EQE) was as high as 28% at 400 nm and 7% at 900 nm, indicating that there was a significant photocurrent contribution from BTPF70 in addition to the **P1** absorption [63].

To increase the solubility, branched alkyl side chains were introduced to the TQ segment or phenylene unit in TQ by the same group [64]. However, the band gaps of resulting polymers increase to 1.3 eV and 1.5 eV respectively, and the photovoltaic performance was inferior. The reason for this is still not clear, but it could be that the poor morphology of the blend films, or the large steric hindrance between the polymers, reduces the charge transfer ability.

Compared with 9-dialkylfluorene, a 2,5-dialkoxyphenylene unit is a stronger electron donor, owing to the electron-donating properties of the alkoxyl group. As a result, **P2** has a lower band gap (~1.0 eV) than **P1**. A BHJ type PSC, based on a **P2**:PCBM mixture, exhibited V_{OC} of 0.34 V, J_{SC} of 3.26 mA cm^{-2}, fill factor (FF) of 0.34, and PCE of 0.38%, with monochromatic photoresponse up to 1.2 μm [65]. For further optimizing the electron-rich group, **P3** was designed and synthesized, in which the carbazole contains a triarylamine unit [66]. The LUMO and HOMO energy levels of **P3** were −3.7 and −4.8 eV, respectively, and the high-lying LUMO energy level ensured effective photoinduced charge transfer to PCBM. The fluorescence of **P3** was almost fully quenched when 6% w/w of PCBM was mixed into films of the polymer. PSCs using 1:1 w/w blends of **P3** and PCBM as the active layers exhibited PCE of 0.61% and a photoresponse up to 1.2 μm.

P4, a polymer of the TQ unit with only bithiophene segment as spacer, was reported by Janssen and coworkers in 2009 [67]. Four 2-ethylhexyl side chains were introduced to the phenyl group to increase the solubility of the resulting polymer. **P4** exhibits a very small band gap of only 0.94 eV. A BHJ type PSC, based on **P4** and a higher fullerene derivative ($PC_{84}BM$), provides a photoresponse up to 1.3 μm with EQE of <1% in the region of 600–1300 nm.

All of these TQ-based μmR-polymers in Scheme 3 showed rather poor photovoltaic performance, having PCEs of less than 1%. This is mainly due to the low EQE values in the NIR region. By changing the donor segment (e.g., to DBS, CPDT, DTS, or DTP mentioned above), the absorption spectra should be extended to the micrometer range, owing to the strong electron-accepting ability of TQ. Therefore, new TQ-based μmR-polymers should still be possible. However, other criteria must be satisfied, such as a suitable LUMO energy level to ensure effective photoinduced charge transfer to PCBM, good solubility and miscibility with PCBM to obtain a uniform blend film, and a high absorption coefficient in the NIR region.

2.2. TP-based and PQ-based μmR-polymers

Scheme 4 shows four μmR-polymers based on TP or PQ units. Polymers **P5** was synthesized by Janssen and coworkers in 2006 from corresponding dibrominated monomer via a Yamamoto condensation polymerization using bis(1,5-cyclooctadiene) nickel(0) ($Ni(COD)_2$) as the catalyst [53]. The UV–vis spectra of **P5**

Table 1
Device characteristics of PSCs based on μmR-polymers.

Polymer	Onset of absorption in film	LUMO/HOMO (eV/eV)	Donor/acceptor ratio (wt/wt)	V_{OC} (V)	J_{SC} (mA cm^{-2})	FF	PCE	Ref.
P1	1000 nm	−3.9/−5.1	PCBM (1:4)	0.69	0.53	0.47	0.17%	[62]
			BTPF (1:4)	0.54	1.76	0.32	0.3%	
			BTPF70 (1:4)	0.58	3.4	0.35	0.7%	[63]
P2	1200 nm		PCBM (1:4)	0.34	3.26	0.34	0.38%	[65]
P3	1200 nm	−3.7/−4.8	PCBM	0.41	5.16	0.29	0.61%	[66]
P4	1300 nm	−3.74/−4.71	PCBM (1:4)	0.37	0.45	0.46	0.08%	[67]
			$PC_{84}BM$ (1:4)	0.10	0.28	0.35	0.01%	
P5	1034 nm		PCBM	0.56	3.1	0.58	1.1%	[53]
P6	1200 nm	−4.1/−5.0	PCBM	~0.2				[82]
P7	1030 nm	−3.96/−5.73	$PC_{70}BM$ (1:3)	0.66	1.5	0.50	0.5%	[59]
P8	1130 nm	−3.90/−5.64	$PC_{70}BM$ (1:3)	0.52	7.3	0.54	2.1%	
P9	1220 nm	−3.59/−4.71	PCBM (1:1)	0.35	0.83	0.39	0.11%	[57]
P10	1030 nm	−3.5/−5.1	$PC_{70}BM$ (1:2)	0.41	2.33	0.36	0.35%	[58]
P11	1130 nm	−3.4/−5.0	$PC_{70}BM$ (1:2)	0.19	1.04	0.28	0.05%	
P12	1380 nm	−3.6/−4.9	$PC_{70}BM$ (1:2)	0.22	1.45	0.31	0.09%	
P13	1100 nm	−3.64/−5.02	PCBM (1:1)	0.44	4.47	0.57	1.12%	[43]
P14	1100 nm	−3.63/−4.90	$PC_{70}BM$ (1:2)	0.38	14.87	0.48	2.71%	[44]
			$PC_{70}BM$ (1:1.5)	0.40	17.55	0.50	3.48%	[45]
P15	1100 nm	−3.56/−4.86	$PC_{70}BM$ (1:1.5)	0.42	22.65	0.52	4.99%	
P16	1000 nm	−3.76/−5.04	$PC_{70}BM$ (1:2)	0.57	8.9	0.59	3.0%	[83]
P17	1055 nm	−3.63/−4.90	$PC_{70}BM$ (1:2)	0.66	13.7	0.66	6.05%	[84]

in solid state revealed that optical absorption extended into the NIR region with onsets of 1034 nm.

The **P5**:PCBM photovoltaic devices exhibited V_{OC} of 0.56 V, J_{SC} of 3.1 mA cm^{-2}, FF of 0.58, and PCE of 1.1% under white light illumination (75 mW cm^{-2}). The higher V_{OC} value for **P5**:PCBM arises from the lower-lying HOMO energy level, and the higher J_{SC} can be attributed to the more uniform film morphology and more intimate mixing of **P5**:PCBM. Interestingly, photovoltaic devices with active layers prepared by depositing an additional quantity of mixed **P5**:PCBM solution on top of the drying layer during spin coating exhibited a much higher EQE in the NIR region. The EQE of these "doubled layer" devices exceeds 15% in the 700–900 nm region. The reason for this enhancement is not clear, but this result reveals a unique possibility to optimize PSC devices.

A simple homopolymer of TP, poly(thieno[3,4-*b*]pyrazine) (**P6**), also showed strong absorption properties in the NIR region [82]. The EQE response of devices based on **P6**:PCBM exhibited maxima at 450 and 925 nm, with an absorption onset up to 1200 nm for post-annealed devices. However, the value of the EQE was low (3–6%) and the overall performance was consequently low, probably because the low-lying LUMO energy level prevented efficient photoinduced charge transfer.

Two high molecular weight PQ-based copolymers, **P7** and **P8** (Scheme 4), were synthesized by the Stille coupling reaction (M_n = 75,000 and 100,000 for **P7** and **P8**, respectively) [59]. The optical band gaps, determined by the onset of the absorption spectra of the films, were 1.2 eV for **P7** and 1.1 eV for **P8**. For the films, the maximum absorption peak at the long wavelength of **P8**

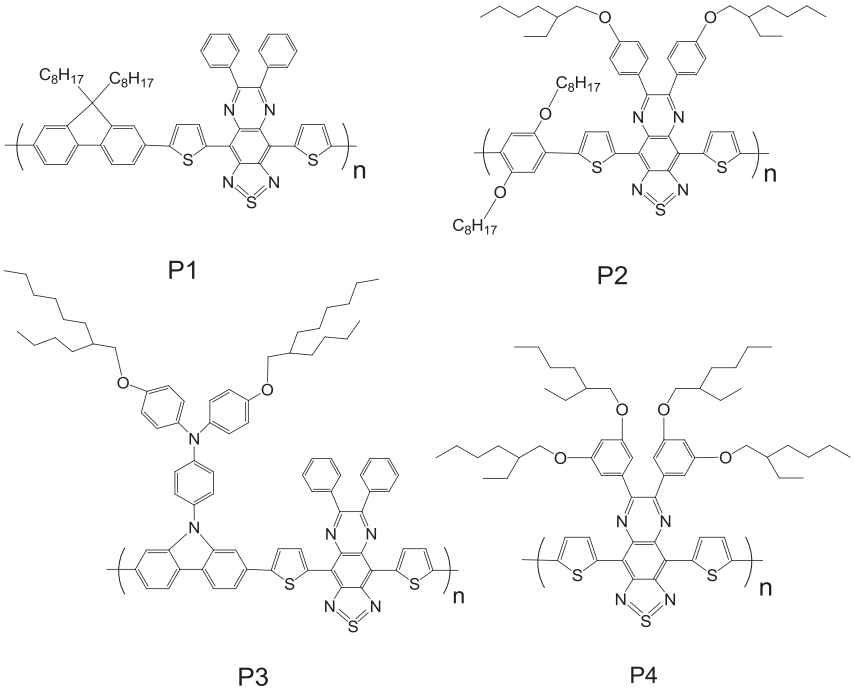

Scheme 3. Reported TQ-based μmR-polymers.

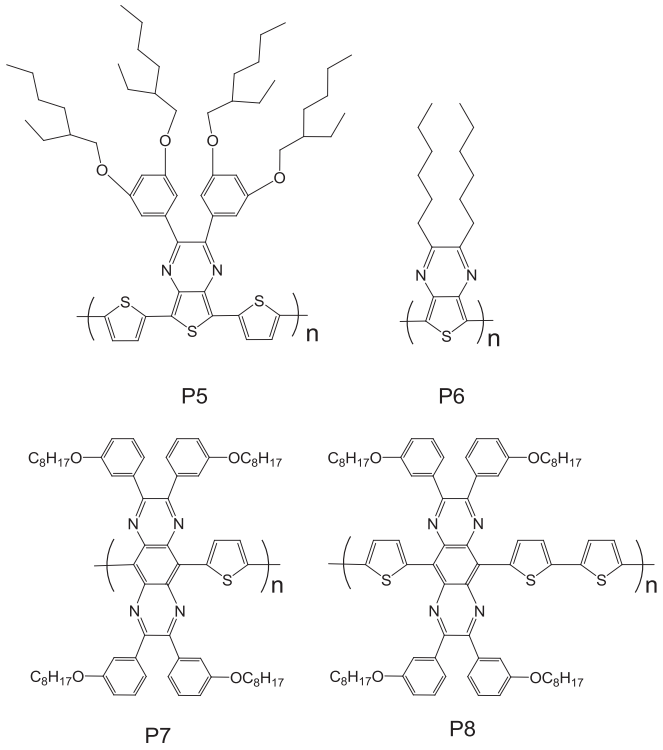

Scheme 4. Two TP-based (P5, P6) and two PQ-based (P7, P8) μmR-polymers.

showed a large redshift, approximately 90 nm, and an increase in intensity. Both of these properties indicate good intermolecular ordering in the solid state, probably due to the longer oligothiophene units. Photovoltaic devices created with **P8**:$PC_{70}BM$ exhibited V_{OC} of 0.52 V, J_{SC} of 7.3 mA cm^{-2}, FF of 0.54, and PCE of 2.1%. The J_{SC} value was enhanced compared with that of a similar **P7**:PCBM device (3.5 mA cm^{-2}), indicating that the charge transfer between **P8** and $PC_{70}BM$ is effective and thus that the energy offset between the LUMO levels of **P8** and $PC_{70}BM$ (0.22 eV) was sufficient. The increase in J_{SC} could be also attributed to the smaller domain size of **P8**:$PC_{70}BM$ blend films.

2.3. TT-based μmR-polymers

Scheme 5 shows four kinds of TT-based copolymers. **P9** was synthesized by Cao and coworkers [57], which had good solution processability, and the film of the polymer absorbed light in the 330–1220 nm region. The LUMO and HOMO energy levels of **P9** were −3.59 eV and −4.71 eV, respectively, with an electrochemical band gap of 1.12 eV. The PSCs based on a **P9**:PCBM blend had V_{OC} of 0.35 V, J_{SC} of 0.83 mA cm^{-2}, and FF of 38.6% under AM 1.5 irradiation (100 mW cm^{-2}), with the photocurrent response wavelengths extending to about 1100 nm. Although the photovoltaic performance was not high, **P9** was used in polymer photodetectors with high sensitivity in their wide spectral response from 300 to 1450 nm [81].

In 2012, Jenekhe and coworkers synthesized a series of TT-based μmR-polymers with optical band gap of 1.2 eV (**P10**), 1.1 eV (**P11**) and 0.9 eV (**P12**) [58]. Although these three polymers showed high FET mobility in the range of 6.1×10^{-4}–4.6×10^{-3} cm^2 V^{-1} s^{-1}, the PCEs were relatively low (<0.35%). The high-lying HOMO energy levels of these polymers resulted in small V_{OC} of 0.19–0.36 V, and the poor quality of the spin-coated polymer/fullerene blend films could explain the low fill factor and PCE of the solar cells.

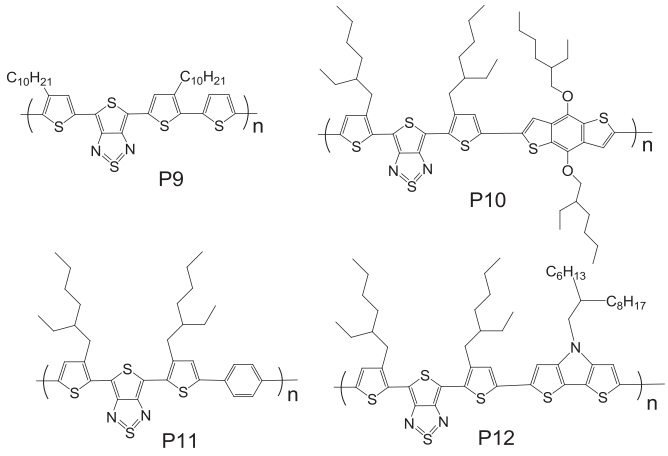

Scheme 5. Four TT-based μmR-polymers.

2.4. DPP-based μmR-polymers

The above-mentioned μmR-polymers exhibit low J_{SC} and poor photovoltaic performance, mainly due to the weak absorption coefficient in near-infrared region and low-lying LUMO energy levels. From 2009, with a new electron-deficient building block, diketopyrrolopyrrole (DPP) was introduced to μmR-polymers design, and large improvements in terms of J_{SC} and PCEs were achieved.

DPP derivatives were first obtained as by-products by Farnum et al. in 1974 [85] and commercialized as high-performance pigments with exceptional light, weather and heat stability. The first DPP-based photovoltaic polymer was reported by Janssen et al. in 2008 [86]. Since then, extensive device engineering has resulted in a number of D–A type, DPP-containing copolymers that have been used in PSCs to achieve PCEs above 5% [87–90]. On the other hand, dithieno[3,2-*b*:2′,3′-*d*]pyrrole (DTP), as a planar building block with strong electron-donating ability, has been first studied for use in D–A type photovoltaic polymers in 2008 [42]. The design of low band gap polymers that combine DTP and electron-deficient acceptor segments has attracted much attention, owing to their tunable optical and electronic properties. In 2009, our group copolymerized DTP with DPP to obtain copolymer **P13** (Scheme 6). **P13** has an absorption band in the long wavelength region, two absorption peaks at 780 nm and 847 nm, and an onset absorption of 1.1 μm [43]. The absorption coefficient of **P13** in $CHCl_3$ solutions is 6.28×10^4 L mol^{-1} cm^{-1} at the absorption maxima. Photovoltaic devices based on **P13**:PCBM exhibit V_{OC} of 0.44 V, J_{SC} of 4.47 mA cm^{-2}, FF of 0.57, and PCE of 1.12%.

Numerous researchers have shown that side chains in conjugated polymers can affect their photovoltaic performance. Thus, we synthesized **P14** (Scheme 6) by changing the alkyl chain in the diketopyrrolopyrrole segment of **P13** from 2-ethylhexyl to n-butyl. **P14** also has a broad absorption band in the range of 500–1100 nm with a tail extending to 1.3 μm. The full width at half-maximum of **P14** film is 324 nm, nearly double that of P3HT film (158 nm). Since the same energy bandwidth would produce a larger width in the wavelength scale, a lower band gap polymer can collect a broader photon flux range. BHJ type PSCs with device configuration of ITO/PEDOT:PSS/**P14**:$PC_{70}BM$(1:2 w/w)/LiF/Al, have a broad photocurrent response wavelength range from 300 nm to 1.1 μm, and high J_{SC} of 14.87 mA cm^{-2}, and PCE of 2.71% were achieved. Compared with the PSC with **P14**:PCBM units, those based on **P14**:$PC_{70}BM$ have higher EQE values, 30–40% in the 450–850 nm range, which contributed to the improvement of J_{SC} from 11.31 mA cm^{-2} to 14.87 mA cm^{-2} [44].

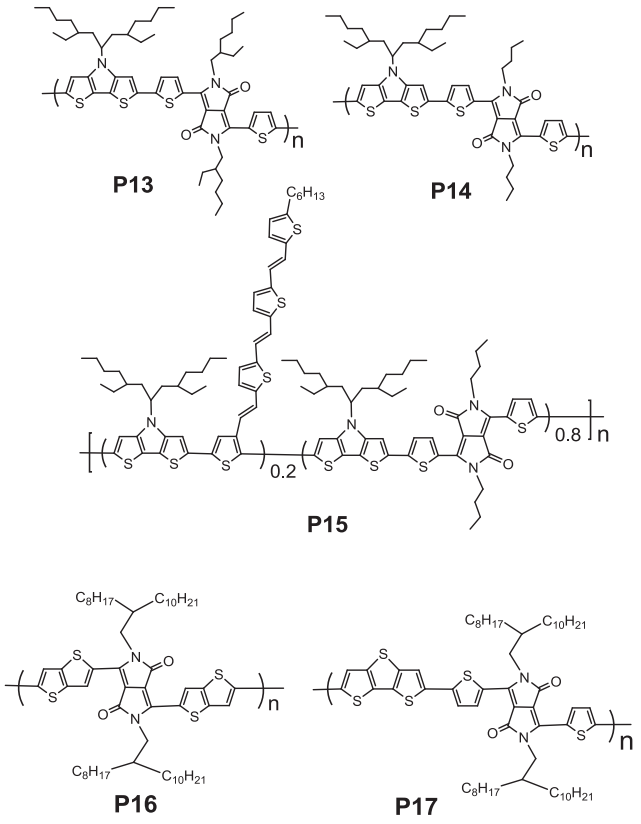

Scheme 6. Five DPP-based μmR-polymers.

The above-mentioned polymers were based on common D–A type polymer design strategies, which include (1) synthesizing novel building blocks or combinations of building blocks, (2) introducing π-spacers for D–π–A polymers, (3) optimizing the alkyl side chains to balance the crystallinity and solubility, and (4) introducing substituents, for example fluorine, to tune the energy levels. However, designing new materials by these methods is rapidly reaching its limits. Therefore, we adopt an alternative approach to designing D–A polymers by introducing a conjugated tris(thienylenevinylene) (TTV) side chain. We utilized this method to modify **P14** and got new polymer of **P15** [45]. The TTV side chain show negligible effect on the absorption spectra and energy levels, but largely improve the photovoltaic performance. By using blend solvents of chloroform and dichlorobenzene, the film morphology can be improved, compared with that from pristine chloroform (Fig. 1). A 43% improvement in the PCE was observed for the **P15**:$PC_{70}BM$ device (4.99%) compared with the P15:$PC_{70}BM$ device (3.48%). In particular, J_{SC} increased from 17.55 mA cm^{-2} to 22.65 mA cm^{-2} after the TTV side chains were introduced, which is the highest J_{SC} reported for a PSC to date. The improvement in EQE over the whole absorption region was observed for the **P15**:$PC_{70}BM$ system compared with the **P14**:$PC_{70}BM$ system, with high value (>0.5) from 400–900 nm (Fig. 2). Because this method of introducing conjugated side chain is also effective for other D–A type polymer, we believe this approach could provide a new general method for designing high-performance D–A photovoltaic polymers.

It is worth noting that introduction of the TTV side chain was also effective to improve the performance of other D–A polymers such as copolymer of benzo[1,2-*b*;3,4-*b*′]dithiophene (BDT) and thieno[3,4-*c*]pyrrole-4,6-dione (TPD). We speculate that the introduction of the TTV side chain improves the charge separation efficiency at the polymer/$PC_{70}BM$ interface. The presence of the

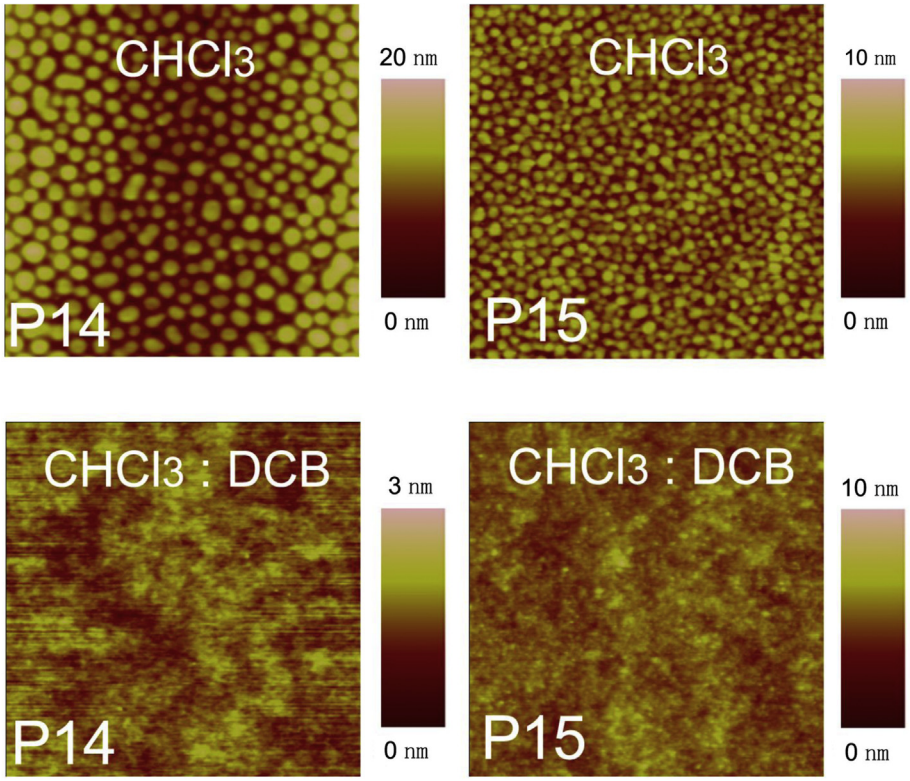

Fig. 1. AFM height images (4 μm × 4 μm) of polymer:$PC_{70}BM$ blend films, spin-coated from $CHCl_3$ solution and from $CHCl_3$ solution with *o*-dichlorobenzene (DCB) additives.

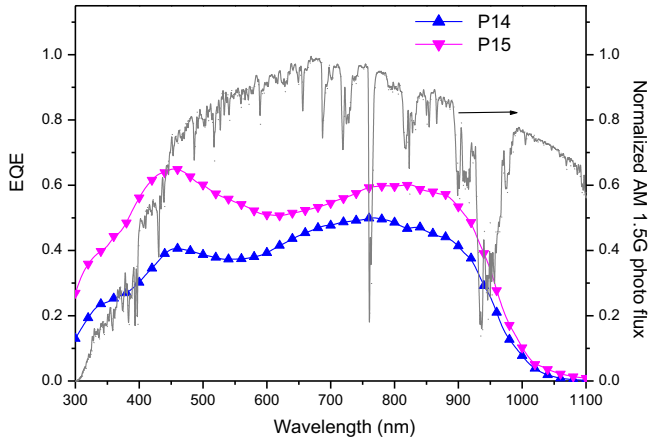

Fig. 2. EQE curves of PSCs based on the **P14** and **P15**. The normalized AM1.5 photon flux spectrum is also shown for comparison.

conjugated π-system may enhance the coupling between the photoexcited state of the polymer and the charge separated state, assuming that the TTV side chains exist at the polymer-fullerene interface (Fig. 3). Of course, the complexity of the BHJ structures in PSCs and the difficulty in analyzing the polymer/fullerene interface mean that the role of the conjugated side chain requires further investigation.

Although the **P15** showed the highest J_{SC}, the V_{OC} was as low as 0.42 V, which is due to the high HOMO energy levels (4.86 eV). In order to get DPP-based μmR-polymers with higher V_{OC}, **P16** and **P17** were designed and synthesized. **P16** is a thieno[3,2-*b*]thiophene-DPP based copolymer with relatively low HOMO energy level of 5.04 eV. Photovoltaic devices created with **P16**:$PC_{70}BM$ exhibits V_{OC} of 0.57 V, J_{SC} of 8.9 mA cm^{-2}, FF of 0.59, and PCE of 3.0%. Further changing the donor building block to dithieno[3,2-*b*:2′,3′-*d*]thiophene (DTT), the resulting polymer, **P17** shows maximum absorption at 802 nm and the absorption onset at 1015 nm in CF solution, while the thin film spectrum exhibits slightly extended onset at 1055 nm. **P17** shows an outstanding hole mobility of 0.60 $cm^2 V^{-1} s^{-1}$ and low-lying HOMO energy levels (5.19 eV). A PCE of 6.05% with J_{SC} of 13.7 mA cm^{-2}, V_{OC} of 0.66 V, and FF of 66.1% were achieved by using **P17**:$PC_{70}BM$ as active layer. These results demonstrate large potential of DPP building block for the design of μmR-polymers.

The success of DPP-based μmR-polymers should attribute to several factors, including the strong absorption in near-infrared region with high absorption coefficient, higher hole mobility, the suitable LUMO energy levels for efficient photoinduced charge transfer to fullerene and good miscibility with fullerene derivatives.

2.5. *n-Type μmR-polymers*

All the above μmR-polymers are p-type polymers, which are blended with fullerene derivatives for photovoltaic applications. Despite this remarkable success of polymer:fulerene blend solar cells, the need for high purity fullerene derivatives, low light absorption in the long wavelength region and the metastable morphology of the fullerene-based BHJs mean that new n-type materials are required.

After almost two decades investigation, four types of n-type polymers containing the electron-deficient groups cyano (CN) [91–93], 2,1,3-benzothiadiazole (BT) [94–96], perylene diimide (PDI) [97–99], and naphthalene diimide (NDI) [100–103] have been recognized as important photovoltaic materials and the highest PCEs for devices based on these four types of polymers are 2.0% [93], 2.7% [96], 2.2% [99], and 1.6% [103], respectively, after intensive device optimization.

A promising advantage of all-polymer solar cells is that the absorption spectra can be modulated individually, thus development of n-type μmR-polymers is vital to utilize most portion of the sunlight. By copolymerization PDI with DTP and introduction of a thiophene unit as a spacer, we synthesized an n-type μmR-polymer **P18** (Scheme 7) [98]. The absorption of **P18** in film extended to over 1 μm, and the LUMO and HOMO energy levels were −4.00 eV and −5.27 eV, respectively. However, owing to the poor solubility of **P18**, the photovoltaic performance was poor in comparison with other n-type polymers. Another n-type μmR-polymer, **P19**, is based on NDI and CPDT building blocks with thiophene as spacer. The LUMO and HOMO energy levels were −4.15 eV and −5.35 eV, respectively. A PCE of 1.1% with J_{SC} of 2.43 mA cm^{-2}, V_{OC} of 0.63 V, and FF of 70% were achieved by using P3HT as the donor material and optimization of the processing solvent. It was found that by suppressing

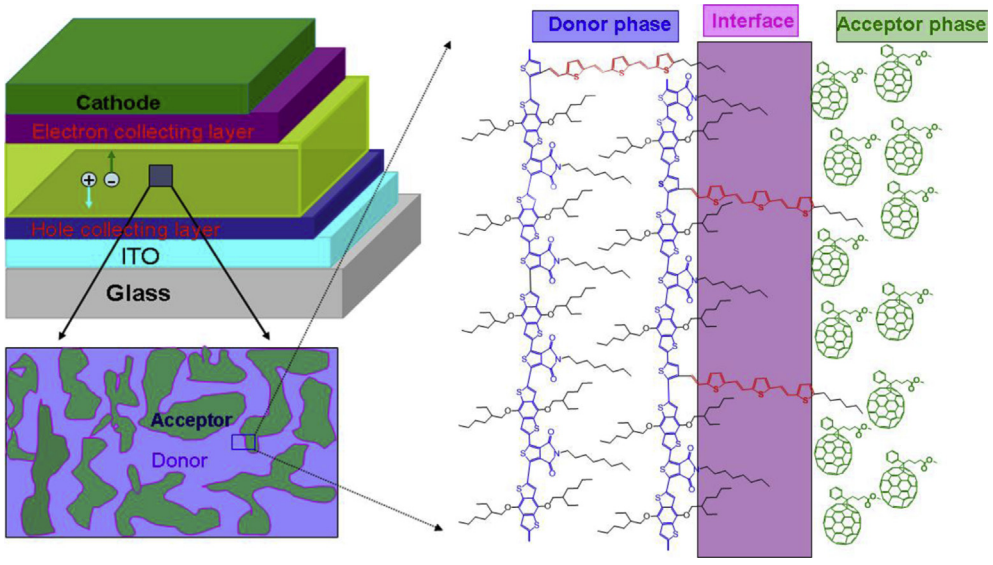

Fig. 3. Schematic diagram of the BHJ structure solar cell. Conjugated side chains placed at the interface are hypothesized to improve the charge separation efficiency.

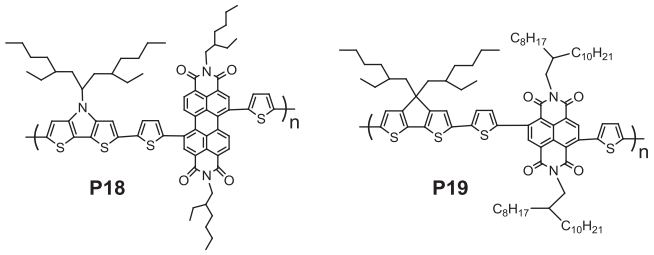

Scheme 7. PDI and NDI-based n-type μmR-polymers.

the aggregation of **P19** at the early stage of film formation, the intermixing of the donor and acceptor component is improved, thereby allowing efficient harvesting of photogenerated excitons at the donor–acceptor heterojunction. Furthermore, correlations between the macroscopic absorption and solar cell performance were also investigated.

3. Conclusion and outlook

In this review, we have summarized the recent works on photovoltaic polymers with photocurrent response extending over 1 μm. The band gap can be tuned by using strong ICT from an electron-rich segment to an electron-deficient segment in the polymer backbone. Fine-tuning of the LUMO and HOMO energy levels of μmR-polymers by structural modification is critical, as doing so can improve V_{OC} and simultaneously enable effective photoinduced charge transfer from the polymer to the acceptor. The absorption coefficient is another important parameter, which ensures that the thin active layer in PSCs can absorb a large proportion of the solar spectrum. Moreover, the morphology of the active layer (polymer:PCBM blend film) is critical for the performance of BHJ cells. If there are large domains and significant phase separation in the active layer, the number of interfaces for efficient charge separation will be reduced. As has been shown, the highest PCE, J_{SC} and EQE for the PSCs based on the presented μmR-polymers reached 6%, 22 mA cm^{-2} and 60% respectively. We can expect to find μmR-polymers that achieve even higher J_{SC} values and better performance in PSCs after material design and device optimization.

A promising application of μmR-polymers is tandem photovoltaic devices. Considering V_{OC} for a tandem cell is equal to the sum of V_{OC} for the two individual cells and the current is limited by whichever cell has the lowest value. Therefore, although there has been great success in producing PSCs with photocurrent responses below 700 nm, there will be an increasing need for highly efficient μmR-polymers materials to utilize sunlight above 700 nm as the manufacturing technology for tandem cells matures. Moreover, because some μmR-polymers show little absorption in the visible region, they may have the potential to create semitransparent PSCs, which are attractive for application in solar cell windows.

References

[1] Brabec CJ, Sariciftci NS, Hummelen JC. Adv Funct Mater 2001;11(1):15–26.
[2] Winder C, Sariciftci NS. J Mater Chem 2004;14(7):1077–86.
[3] Scharber MC, Mühlbacher D, Koppe M, Denk P, Waldauf C, Heeger AJ, et al. Adv Mater 2006;18(6):789–94.
[4] Thompson BC, Frechet JM. Angew Chem Int Ed 2008;47(1):58–77.
[5] Dennler G, Scharber MC, Brabec CJ. Adv Mater 2009;21(13):1323–38.
[6] Brabec CJ, Gowrisanker S, Halls JJ, Laird D, Jia S, Williams SP. Adv Mater 2010;22(34):3839–56.
[7] Boudreault P-LT, Najari A, Leclerc M. Chem Mater 2011;23(3):456–69.
[8] Son HJ, Carsten B, Jung IH, Yu L. Energy Environ Sci 2012;5(8):8158–70.
[9] Yu G, Gao J, Hummelen JC, Wudl F, Heeger AJ. Science 1995;270(5243):1789–90.
[10] Ma W, Yang C, Gong X, Lee K, Heeger AJ. Adv Funct Mater 2005;15(10):1617–22.
[11] Li G, Shrotriya V, Huang J, Yao Y, Moriarty T, Emery K, et al. Nat Mater 2005;4(11):864–8.
[12] Li Y, Zou Y. Adv Mater 2008;20(15):2952–8.
[13] Zhou EJ, He C, Tan ZA, Yang CH, Li YF. J Polym Sci, Part A: Polym Chem 2006;44(16):4916–22.
[14] Zhou EJ, Hou JH, Yang CH, Li YF. J Polym Sci, Part A: Polym Chem 2006;44(7):2206–14.
[15] Zhou EJ, Tan ZA, Huo LJ, He YJ, Yang CH, Li YF. J Phys Chem B 2006;110(51):26062–7.
[16] Zhou EJ, Tan ZA, Yang CH, Li YF. Macromol Rapid Commun 2006;27(10):793–8.
[17] Zhou EJ, Tan ZA, He YJ, Yang CH, Li YF. J Polym Sci, Part A: Polym Chem 2007;45(4):629–38.
[18] Zhou EJ, Tan ZA, Yang Y, Huo LJ, Zou YP, Yang CH, et al. Macromolecules 2007;40(6):1831–7.
[19] Liang Y, Yu L. Acc Chem Res 2010;43(9):1227–36.
[20] Zhou H, Yang L, You W. Macromolecules 2012;45(2):607–32.
[21] Zhang ZG, Wang JJ. Mater Chem 2012;22(10):4178–87.
[22] Svensson M, Zhang F, Veenstra SC, Verhees WJ, Hummelen JC, Kroon JM, et al. Adv Mater 2003;15(12):988–91.
[23] Liu J, Choi H, Kim JY, Bailey C, Durstock M, Dai L. Adv Mater 2012;24(4):538–42.
[24] Chen M-H, Hou J, Hong Z, Yang G, Sista S, Chen L-M, et al. Adv Mater 2009;21(42):4238–42.
[25] Wang E, Wang L, Lan L, Luo C, Zhuang W, Peng J, et al. Appl Phys Lett 2008;92(3):033307.
[26] Boudreault P-LT, Michaud A, Leclerc M. Macromol Rapid Commun 2007;28(22):2176–9.
[27] Allard N, RdB Aïch, Gendron D, Boudreault P-LT, Tessier C, Alem S, et al. Macromolecules 2010;43(5):2328–33.
[28] Blouin N, Michaud A, Leclerc M. Adv Mater 2007;19(17):2295–300.
[29] Blouin N, Michaud A, Gendron D, Wakim S, Blair E, Neagu-Plesu R, et al. J Am Chem Soc 2008;130(2):732–42.
[30] Chu T-Y, Alem S, Tsang S-W, Tse S-C, Wakim S, Lu J, et al. Appl Phys Lett 2011;98(25):253301.
[31] Mühlbacher D, Scharber M, Morana M, Zhu Z, Waller D, Gaudiana R, et al. Adv Mater 2006;18(21):2884–9.
[32] Peet J, Kim JY, Coates NE, Ma WL, Moses D, Heeger AJ, et al. Nat Mater 2007;6(7):497–500.
[33] Lee JK, Ma WL, Brabec CJ, Yuen J, Moon JS, Kim JY, et al. J Am Chem Soc 2008;130(11):3619–23.
[34] Albrecht S, Janietz S, Schindler W, Frisch J, Kurpiers J, Kniepert J, et al. J Am Chem Soc 2012;134(36):14932–44.
[35] Hou J, Chen HY, Zhang S, Li G, Yang Y. J Am Chem Soc 2008;130(48):16144–5.
[36] Coffin RC, Peet J, Rogers J, Bazan GC. Nat Chem 2009;1(8):657–61.
[37] Chen HY, Hou J, Hayden AE, Yang H, Houk KN, Yang Y. Adv Mater 2010;22(3):371–5.
[38] Amb CM, Chen S, Graham KR, Subbiah J, Small CE, So F, et al. J Am Chem Soc 2011;133(26):10062–5.
[39] Gendron D, Morin P-O, Berrouard P, Allard N, Aïch BR, Garon CN, et al. Macromolecules 2011;44(18):7188–93.
[40] Small CE, Chen S, Subbiah J, Amb CM, Tsang S-W, Lai T-H, et al. Nat Photonics 2011;6:115–20.
[41] Fei Z, Shahid M, Yaacobi-Gross N, Rossbauer S, Zhong H, Watkins SE, et al. Chem Commun 2012;48(90):11130–2.
[42] Zhou EJ, Nakamura M, Nishizawa T, Zhang Y, Wei QS, Tajima K, et al. Macromolecules 2008;41(22):8302–5.
[43] Zhou EJ, Yamakawa S, Tajima K, Yang CH, Hashimoto K. Chem Mater 2009;21(17):4055–61.
[44] Zhou EJ, Wei QS, Yamakawa S, Zhang Y, Tajima K, Yang CH, et al. Macromolecules 2010;43(2):821–6.
[45] Zhou EJ, Cong JZ, Hashimoto K, Tajima K. Energy Environ Sci 2012;5(12):9756–9.
[46] Gadisa A, Mammo W, Andersson LM, Admassie S, Zhang F, Andersson MR, et al. Adv Funct Mater 2007;17(18):3836–42.
[47] Wang E, Hou L, Wang Z, Hellstrom S, Zhang F, Inganas O, et al. Adv Mater 2010;22(46):5240–4.
[48] Zhou EJ, Cong JZ, Tajima K, Hashimoto K. Chem Mater 2010;22(17):4890–5.
[49] Zhang Y, Zou J, Yip H-L, Chen K-S, Zeigler DF, Sun Y, et al. Chem Mater 2011;23(9):2289–91.
[50] Chen H-C, Chen Y-H, Liu C-C, Chien Y-C, Chou S-W, Chou P- T. Chem Mater 2012;24(24):4766–72.
[51] Zhang F, Perzon E, Wang X, Mammo W, Andersson MR, Inganäs O. Adv Funct Mater 2005;15(5):745–50.
[52] Ashraf RS, Shahid M, Klemm E, Al-Ibrahim M, Sensfuss S. Macromol Rapid Commun 2006;27(17):1454–9.
[53] Wienk MM, Turbiez MGR, Struijk MP, Fonrodona M, Janssen RAJ. Appl Phys Lett 2006;88(15):153511.
[54] Zhang F, Mammo W, Andersson LM, Admassie S, Andersson MR, Inganäs O. Adv Mater 2006;18(16):2169–73.
[55] Zhou EJ, Cong JZ, Yamakawa S, Wei QS, Nakamura M, Tajima K, et al. Macromolecules 2010;43(6):2873–9.
[56] Rasmussen SC, Schwiderski RL, Mulholland ME. Chem Commun 2011;47(41):11394–410.

[57] Xia Y, Wang L, Deng X, Li D, Zhu X, Cao Y. Appl Phys Lett 2006;89(8):081106.
[58] Hwang Y-J, Kim FS, Xin H, Jenekhe SA. Macromolecules 2012;45(9):3732–9.
[59] Wang E, Hou L, Wang Z, Hellström S, Mammo W, Zhang F, et al. Org Lett 2010;12(20):4470–3.
[60] Zhang F, Bijleveld J, Perzon E, Tvingstedt K, Barrau S, Inganäs O, et al. J Mater Chem 2008;18(45):5468–74.
[61] Zoombelt AP, Fonrodona M, Turbiez MGR, Wienk MM, Janssen RAJ. J Mater Chem 2009;19(30):5336–42.
[62] Wang X, Perzon E, Delgado JL, de La Cruz P, Zhang F, Langa F, et al. Appl Phys Lett 2004;85(21):5081–3.
[63] Wang X, Perzon E, Oswald F, Langa F, Admassie S, Andersson MR, et al. Adv Funct Mater 2005;15(10):1665–70.
[64] Wang X, Perzon E, Mammo W, Oswald F, Admassie S, Persson N-K, et al. Thin Solid Films 2006;511-512:576–80.
[65] Perzon E, Zhang F, Andersson M, Mammo W, Inganäs O, Andersson MR. Adv Mater 2007;19(20):3308–11.
[66] Yi H, Johnson RG, Iraqi A, Mohamad D, Royce R, Lidzey DG. Macromol Rapid Commun 2008;29(22):1804–9.
[67] Zoombelt AP, Fonrodona M, Wienk MM, Sieval AB, Hummelen JC, Janssen RA. Org Lett 2009;11(4):903–6.
[68] Bundgaard E, Krebs FC. Macromolecules 2006;39(8):2823–31.
[69] Fan J, Yuen JD, Wang M, Seifter J, Seo JH, Mohebbi AR, et al. Adv Mater 2012;24(16):2186–90.
[70] Oh HS, Kim TD, Koh YH, Lee KS, Cho S, Cartwright A, et al. Chem Commun 2011;47(31):8931–3.
[71] Yuen JD, Fan J, Seifter J, Lim B, Hufschmid R, Heeger AJ, et al. J Am Chem Soc 2011;133(51):20799–807.
[72] Ameri T, Dennler G, Lungenschmied C, Brabec CJ. Energy Environ Sci 2009;2(4):347–63.
[73] Hadipour A, de Boer B, Blom PWM. Org Electron 2008;9(5):617–24.
[74] Gevaerts VS, Furlan A, Wienk MM, Turbiez M, Janssen RAJ. Adv Mater 2012;24(16):2130–4.
[75] Seo JH, Kim DH, Kwon SH, Song M, Choi MS, Ryu SY, et al. Adv Mater 2012;24(33):4523–7.
[76] Sista S, Park MH, Hong Z, Wu Y, Hou J, Kwan WL, et al. Adv Mater 2010;22(3):380–3.
[77] Kouijzer S, Esiner S, Frijters CH, Turbiez M, Wienk MM, Janssen RAJ. Adv Energy Mater 2012;2(8):945–9.
[78] Dou L, You J, Yang J, Chen C-C, He Y, Murase S, et al. Nat Photonics 2012;6(3):180–5.
[79] Kim JY, Lee K, Coates NE, Moses D, Nguyen TQ, Dante M, et al. Science 2007;317(5835):222–5.
[80] You J, Dou L, Yoshimura K, Kato T, Ohya K, Moriarty T, et al. Nat Commun 2013;4:1446.
[81] Gong X, Tong M, Xia Y, Cai W, Moon JS, Cao Y, et al. Science 2009;325(5948):1665–7.
[82] Wen L, Duck BC, Dastoor PC, Rasmussen SC. Macromolecules 2008;41(13):4576–8.
[83] Bronstein H, Chen Z, Ashraf RS, Zhang W, Du J, Durrant JR, et al. J Am Chem Soc 2011;133(10):3272–5.
[84] Jung JW, Liu F, Russell TP, Jo WH. Energy Environ Sci 2012;5(5):6857–61.
[85] Farnum DG, Mehta G, Moore GG, Siegal FP. Tetrahedron Lett 1974;15(29):2549–52.
[86] Wienk MM, Turbiez M, Gilot J, Janssen RAJ. Adv Mater 2008;20(13):2556–60.
[87] Woo CH, Beaujuge PM, Holcombe TW, Lee OP, Fréchet JM. J Am Chem Soc 2010;132(44):15547–9.
[88] Dou L, Gao J, Richard E, You J, Chen CC, Cha KC, et al. J Am Chem Soc 2012;134(24):10071–9.
[89] Dou L, Chang WH, Gao J, Chen CC, You J, Yang Y. Adv Mater 2013;25(6):825–31.
[90] Bijleveld JC, Gevaerts VS, Di Nuzzo D, Turbiez M, Mathijssen SG, de Leeuw DM, et al. Adv Mater 2010;22(35):E242–6.
[91] Halls J, Walsh C, Greenham N, Marseglia E, Friend R, Moratti S, et al. Nature 1995;376:498–500.
[92] Granström M, Petritsch K, Arias A, Lux A, Andersson M, Friend R. Nature 1998;395(6699):257–60.
[93] Holcombe TW, Woo CH, Kavulak DF, Thompson BC, Frechet JM. J Am Chem Soc 2009;131(40):14160–1.
[94] Halls JJ, Arias A, MacKenzie JD, Wu W, Inbasekaran M, Woo E, et al. Adv Mater 2000;12(7):498–502.
[95] McNeill CR, Abrusci A, Zaumseil J, Wilson R, McKiernan MJ, Burroughes JH, et al. Appl Phys Lett 2007;90(19):193506.
[96] Mori D, Benten H, Ohkita H, Ito S, Miyake KACS. Appl Mater Interfaces 2012;4(7):3325–9.
[97] Zhan XW, Tan ZA, Domercq B, An ZS, Zhang X, Barlow S, et al. J Am Chem Soc 2007;129(23):7246–7.
[98] Zhou EJ, Tajima K, Yang CH, Hashimoto KJ. Mater Chem 2010;20(12):2362–8.
[99] Zhou EJ, Cong JZ, Wei QS, Tajima K, Yang CH, Hashimoto K. Angew Chem Int Ed 2011;50(12):2799–803.
[100] Yan H, Chen Z, Zheng Y, Newman C, Quinn JR, Dotz F, et al. Nature 2009;457(7230):679–86.
[101] Hwang Y-J, Ren G, Murari NM, Jenekhe SA. Macromolecules 2012;45(22):9056–62.
[102] Schubert M, Dolfen D, Frisch J, Roland S, Steyrleuthner R, Stiller B, et al. Adv Energy Mater 2012;2(3):369–80.
[103] Zhou EJ, Cong JZ, Zhao MJ, Zhang LZ, Hashimoto K, Tajima K. Chem Commun 2012;48(43):5283–5.

Erjun Zhou received his Ph.D. degree in chemistry from the Institute of Chemistry, Chinese Academy of Sciences (ICCAS) in 2007 under the supervision of Prof. Yongfang Li. Then, he joined the Hashimoto Light Energy Conversion Project, part of the Exploratory Research for Advanced Technology (ERATO) research program at the Japan Science and Technology Agency (JST), as a research scientist from 2007 to 2011. From 2011 to 2013, he worked with Prof. Kazuhito Hashimoto as a postdoctoral fellow at the University of Tokyo. Currently, he is working in RIKEN Center for Emergent Matter Science (CEMS) as a research scientist. His research interests are the design, synthesis, and characterization of organic and polymeric functional materials for optoelectronic and photovoltaic applications.

Keisuke Tajima received his B.S. (1997), M.S. (1999), and Ph.D. degrees (2002) from the University of Tokyo under the direction of Prof. Takuzo Aida. During 2002–2004, he conducted postdoctoral research under the direction of Prof. Samuel I. Stupp at Northwestern University. In 2004, he joined the University of Tokyo as an assistant professor, where he was promoted to lecturer in 2009 and associate professor in 2011. From 2011, he also became a PRESTO researcher at JST. From 2013, he joined RIKEN CEMS as a team leader. His research interests include synthesis of new organic and polymeric materials for application in organic electronic devices such as polymer solar cells.

Kazuhito Hashimoto studied chemistry at the University of Tokyo where he received his B.S. (1978), M.S. (1980), and Ph.D. (1985) degrees. From 1980, he worked at the Institute for Molecular Science as a technical associate and as a research associate. He joined the University of Tokyo as a lecturer in 1989, where he was promoted to associate professor in 1991 and to full professor in 1997. At present, he is a professor in the Department of Applied Chemistry at the University of Tokyo and at the Research Center for Advanced Science and Technology. Furthermore, he is the project leader of the ERATO Hashimoto Light Energy Conversion Project. He has received many awards for his research excellence, including the IBM Science Award (1997), the Nikkei Environmental Technology Award (2004), the Prime Minister Award from the Cabinet Office of Japan (2004), and the Japan Invention Award (2006). His current research interests involve photo-related materials, such as photocatalysts, polymer photovoltaic cells, and microbial solar cells.